



¹⁴C GIRI SAMPLES IN AMS GOLDEN VALLEY: GRAPHITE PREPARATION USING AGE-3 AND ABSORPTION-CATALYTIC SETUP

E V Parkhomchuk^{1,3,4*}  • A V Petrozhitskiy^{1,2,3}  • M M Ignatov^{1,3} • D V Kuleshov^{1,3} • A I Lysikov⁴ • A G Okunev¹ • K A Babina^{3,4} • V V Parkhomchuk^{1,2}

¹Novosibirsk State University, AMS Golden Valley, 2 Pirogova str., Novosibirsk, 630090, Russia

²Budker Institute of Nuclear Physics Siberian Branch Russian Academy of Sciences (BINP SB RAS), 11 Acad. Lavrentiev Ave., Novosibirsk, 630090, Russia

³Institute of Archaeology and Ethnography SB RAS, 17 Acad. Lavrentiev Ave., Novosibirsk, 630090, Russia

⁴Boreskov Institute of Catalysis SB RAS, 5 Acad. Lavrentiev Ave., Novosibirsk, 630090, Russia

ABSTRACT. The AMS Golden Valley laboratory is equipped with two accelerator mass spectrometers: the AMS facility from the Budker Institute of Nuclear Physics (BINP) and the Mini Carbon Dating System (MICADAS-28) from Ionplus AG and two graphitization systems: the Automated Graphitization Equipment (AGE-3) from Ionplus AG and the Absorption-catalytic setup (ACS) developed at the Boreskov Institute of Catalysis (BIC). The ACS was designed for graphite preparation from labeled biomedical samples, dissolved organics, and dissolved or gaseous carbon dioxide but has proven to be suitable for the traditional dating of objects no older than 35,000 years. Here we present two series of AMS data for the samples from Glasgow International Radiocarbon Inter-comparison (GIRI), prepared using AGE-3 and ACS, and then measured on MICADAS-28. The mean value of the background F¹⁴C was 0.0024 ± 0.0009 and 0.012 ± 0.003 for AGE-3 and ACS, respectively, and both methods gave reproducible results for the OXI.

KEYWORDS: AMS, graphitization systems, intercomparison, radiocarbon.

INTRODUCTION

The radiocarbon AMS laboratory in Novosibirsk started its operation in 2011 after installing the 1 MV AMS facility built by the Budker Institute of Nuclear Physics (BINP) (Parkhomchuk and Rastigeev 2011). In the first years of work, graphite targets were made by cryogenic distillation of CO₂ with a subsequent reduction of carbon dioxide to graphite, requiring much time and human resources and, therefore, unsuitable for multiple biomedical samples. However, using AMS in biomedical applications seemed extremely promising (Arjomand 2010; Synal 2013; Parkhomchuk et al. 2022), and we were forced to develop our own graphitization system. The graphitization method using an elemental analyzer to gasify the sample and AGE-3 to reduce the generated CO₂ (Wacker et al. 2010) was available only in Moscow, 3000 km from our laboratory. To simplify and reduce the running costs of the graphitization procedure, we proposed a new approach based on the fast catalytic combustion of the sample followed by “inverted” carbon dioxide purification, which is a one-step CO₂ separation from oxidation products by the selective sorption and subsequent reduction by H₂ (Lysikov et al. 2018). After optimizing parameters such as the amounts of sorbent and sample weight, gas flow rate, types of catalyst and amounts needed for organic matter combustion and CO₂ reduction, and setup automation, the absorption-catalytic setup (ACS) was installed in 2015 (Figure 1) and started to operate together with BINP AMS. The proposed method was found to be reproducible according to the results for the OX-I and OX-II standards measured from 2015 to 2018. This method was successfully used for dating different types of samples, including CO₂ dissolved in natural waters (Novikov et al. 2023) and methane from seeps (Sabrekov et al. 2023), and showed consensus with the data from some other laboratories (Molodin et al. 2019; Rudaya et al. 2020). With the ACS, BINP AMS was applied for studying the penetration of organic aerosols inhaled by laboratory mice at ultra-low

*Corresponding author. Email: ekaterina@catalysis.ru

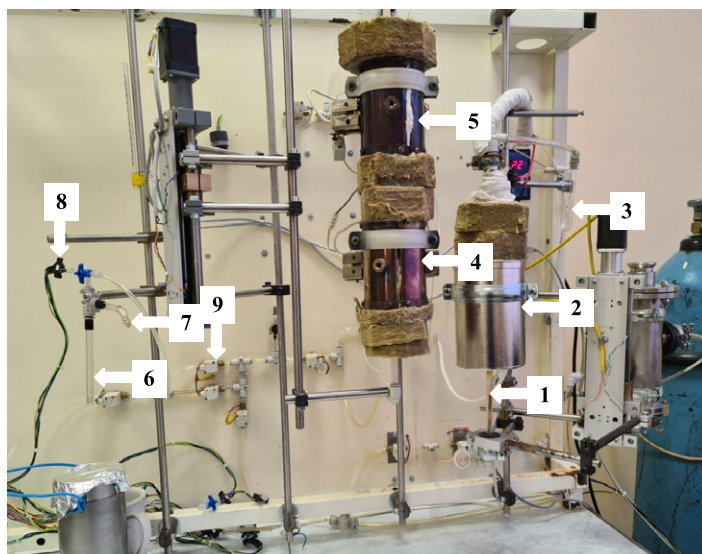


Figure 1 Photograph of the ACS for sample graphitization: 1 – sample placement, 2 – combustion zone, 3 – zone of water vapor freezing; 4 – CO₂ absorption on the CaO, 5 – CO₂ desorption, 6 – CO₂ collecting with liquid nitrogen, 7 – drying zone, 8 – pressure sensor, 9 – valves for automatic procedures: hydrogen addition, evacuation, CO₂ collecting. The furnace for graphitization is not shown.

concentration ca. 10^3 cm^{-3} . For this purpose, we synthesized polystyrene beads composed of radiocarbon-labeled styrene to be tested as model organic aerosols (Parkhomchuk et al. 2016; Parkhomchuk et al. 2019). Since the ACS has proven successful for both ancient and ¹⁴C-enriched samples, we have installed and are currently operating two identical ACSs located 1.5 km apart in order to avoid cross-contamination.

The MICADAS-28 (Synal et al. 2007) with AGE-3 was supplied to Novosibirsk State University (NSU) in December 2019 and on May 29, 2020, based on the Agreement signed by the rector of NSU and the directors of three institutions of the Novosibirsk Scientific Center (the Budker Institute of Nuclear Physics, the Institute of Archeology and Ethnography and the Borekov Institute of Catalysis), AMS Golden Valley was created, with the name given after the place where the Novosibirsk Akademgorodok was founded.

This was the first time that our laboratory participated in the radiocarbon intercomparison. To test all possible toolkits during the Glasgow International Radiocarbon Intercomparison, we conducted three series of experiments: (1) AGE-3 + MICADAS-28, (2) ACS + MICADAS-28, (3) AGE-3 + BINP AMS, using the maximum possible number of samples. This work presents the results of AMS dating of the first and second series. The analysis of the GIRI results of the first and third series of experiments used to reveal the comparative characteristics of BINP AMS and MICADAS-28 can be found in the paper of Petrozhitskiy et al. (2024).

MATERIALS AND METHODS

In November 2021, AMS Golden Valley received two sets of GIRI samples, including a total of seventeen natural substances such as wood, bone, cellulose, humic acid, and barley mash (Table 1). The volume of material in set 1 was sufficient to make a few repeat measurements.

Table 1 Results of GIRI samples graphitized by two devices, AGE-3 and ACS, and then measured on MICADAS-28 together with data on $\delta^{13}\text{C}$ measured by MICADAS-28 and Delta-V-Advantage. F = the measured fraction modern with fractionation correction applied to both the sample and blank samples and corrected for background. Uncertainties represent 1 sigma.

Name/ laboratory ID	Intersection (Scott et al. 2023)	Description	$\delta^{13}\text{C}$, ‰	$\delta^{13}\text{C}$, ‰ MICADAS		F value		Radiocarbon age (BP)		Preliminary consensus GIRI ¹ (Scott et al. 2023)
				AGE-3	ACS	AGE-3	ACS	AGE-3	ACS	
Set 1										
A GV-3799	TIRI A	Barley mash	-26.0	-24.4 -23.0	-24.5	1.1638 ± 0.0030	1.1636 ± 0.0076	—	—	1.1643 ± 0.0075 ⁵
B GV-3800	VIRI U	Humic acid ²	-29.7	-28.9 -29.9	-29.2 -28.0 -29.5	0.2293 ± 0.0008	0.2248 ± 0.0029	11832 ± 29	11991 ± 103	11813 ± 110
C GV-3801		Barley mash	-28.0	-29.3	-27.3 -26.4 -15.8 -37.8	1.0075 ± 0.0041	1.0161 ± 0.0043	—	—	1.0227 ± 0.0072 ⁵
D GV-3802		Humic acid ²	-28.5	-26.7 -27.7	-24.2 -29.3 -30.5	0.6226 ± 0.0017	0.6131 ± 0.0031	3806 ± 22	3930 ± 40	3826 ± 71
E GV-3803	SIRI F,G,H	Dendro-dated wood	-26.0	-23.7 -25.1	-23.6 -22.9	0.9563 ± 0.0025	0.9512 ± 0.0047	359 ± 21	402 ± 40	378 ± 49
F GV-3804		Barley mash	-26.6	-26.2 -27.0	-26.3	1.0174 ± 0.0026	1.0085 ± 0.0069	—	—	1.0162 ± 0.0117 ⁵
G GV-3805	TIRI B FIRI D	Dendro-dated wood	-23.4	-22.0 -21.8	-25.6 -25.8	0.5690 ± 0.0029	0.5673 ± 0.0036	4530 ± 41	4553 ± 51	4523 ± 49
H GV-3806		Dendro-dated wood; single ring	-19.3	-17.1 -18.7	—	0.7592 ± 0.0020	—	2213 ± 21	—	2208 ± 50
I GV-3807		Kauri wood	-22.2	-19.8 -20.5 -21.4 -22.0	—	0.0535 ± 0.0006	—	23518 ± 89	—	23644 ± 168
J GV-3808		Kauri wood	-21.7	-20.9 -20.3 -22.9	-22.7 -22.6	0.0086 ± 0.0003	0.0072 ± 0.0027	38245 ± 314	>35000	38571 ± 886
K(1) ³ GV-3809	TIRI L	Whalebone	-14.8	-15.1 -12.2	-15.6	0.2030 ± 0.0006	0.2009 ± 0.0028	12810 ± 47	12894 ± 113	12780 ± 114
K(2) ⁴ GV-3809				-14.2 -15.6	-15.2					
L GV-3810		Dendro-dated wood; single ring	-19.8	-17.7 -16.8	—	0.7402 ± 0.0072	—	2416 ± 78	—	2241 ± 58

(Continued)

Table 1 (Continued)

Name/ laboratory ID	Intersection (Scott et al. 2023)	Description	$\delta^{13}\text{C}$, ‰	$\delta^{13}\text{C}$, ‰ MICADAS		F value		Radiocarbon age (BP)		
				AGE-3	ACS	AGE-3	ACS	AGE-3	ACS	Preliminary consensus GIRI ¹ (Scott et al. 2023)
Set 1										
M	VIRI O	Dendro-dated cellulose ²	-25.5	-25.1	-22.5	0.9820 ± 0.0027	0.9779 ± 0.0048	146 ± 22	180 ± 39	132 ± 32
GV-3811				-24.1	-20.9					
N		Kauri wood	-22.1	-23.6	-20.4	0.0021 ± 0.0004	0.0005 ± 0.0027	>52000	>35000	0.002146 ± 0.00181 ⁵
GV-3812				-22.9	-20.4					
Q		Dendro-dated wood; single ring	-23.4	-25.6	—	0.9595 ± 0.0027	—	332 ± 22	—	336 ± 46
GV-3813				-24.6	—					
Set 2										
O	FIRI E	Humic acid ²	-29.9	-30.0	-28.7	0.2306 ± 0.0008	0.2256 ± 0.0029	11783 ± 29	11960 ± 104	11826 ± 153
GV-3814				-29.7	-28.7					
P	FIRI H	Dendro-dated wood	-24.4	-23.5	-22.8	0.7584 ± 0.0022	0.7534 ± 0.0041	2221 ± 23	2274 ± 44	2227 ± 62
GV-3815				-24.7	-22.3					

¹— mean value ± stdev²— pretreatment not required³— $\delta^{15}\text{N} = 12.8$ ‰; C/N = 3.2⁴— $\delta^{15}\text{N} = 12.7$ ‰; C/N = 3.2⁵— given as F

Set 2 (samples **O** and **P**) was sufficient to run multiple measurements and to be used for internal quality assurance. Three humic acid samples (**B**, **D**, and **O**) and one cellulose sample (**M**) pre-treated before being sent to the laboratory were graphitized without any pre-treatment, with remaining samples requiring pre-treatment. Eight samples were offered for earlier intercomparisons. The results were sent to Glasgow on April 18, 2022, and our report was presented at the 24th Radiocarbon Conference in September 2022 in Zurich.

Sample Preparation

Wood

Wood samples **H**, **I**, and **P** were subjected to multistage extraction purification on an automatic extraction unit ASETM350 (Accelerated Solvent Extractor - Dionex Corporation): 4 times with C₂H₂Cl₂ : C₂H₅OH = 2 : 1, then 5 times with C₂H₅OH, and 6 times with distilled water until a colorless solution was obtained. The samples were dried at 60°C. Then, delignification was performed by a catalytic method in an acidic medium: 0.15 g of NaWO₄ was dissolved in 40 mL of distilled water, dried wood samples were added to the resulting solution, 4 drops of concentrated sulfuric acid and 40 mL of 1% H₂O₂ were added, heated to 80°C, and kept for 4 hours. Then, the precipitate was separated from the solution, distilled water was added, boiled for 15 minutes, washing was repeated 3 times, 1% H₂O₂ was added, heated to 80°C, kept for 1 hour, and boiled again in distilled water for 15 minutes three times. The catalytic procedure was repeated twice. Then, 0.1 M NaOH solution was added to the precipitate, kept at 70°C for 15 minutes, washed twice with distilled water, poured with 0.1 M NaOH solution, kept at 70°C for 45 minutes, washed twice with distilled water, and poured again with 0.1 M NaOH solution. The precipitate was kept at 70°C for 60 minutes and washed 4 times with distilled water. Next, 1% H₂O₂ was added to the precipitate, kept at 75°C for 1 hour, then at room temperature for 12 hours, and washed twice with distilled water. The procedure was repeated 4 times under the same conditions, except for the NaOH concentration: 0.5 M instead of 0.1 M. Next, the precipitate was treated with 1 M HCl at 80°C for 1 hour and washed 4–5 times until pH = 7. A total of 9.4 mL of distilled water, 600 µl of 10% sodium chlorite, and 400 µl of 1 M HCl were added to the separated samples, kept at room temperature for 4 hours, washed with distilled water 2–3 times, and the procedure was repeated until a colorless solution and snow-white cellulose were obtained. Cellulose was separated from the solution, washed with distilled water about 15 times until the chlorine smell disappeared, and dried at 70°C.

Wood samples **E**, **G**, **J**, and **Q** were subjected to the same cleaning procedure, except for the H₂O₂ concentration during the catalytic treatment was 2.5% for samples **E** and **Q** and 5% for samples **G** and **J**, and the NaOH concentration from 0.5 to 1 M during the repeated alkaline treatment. Lower concentrations were used in case of doubts about the good preservation of the material to prevent the substance from being wasted.

Wood sample **N** also underwent a procedure similar to that described above, except for an additional acid treatment procedure (the precipitate was treated with 1 M HCl at 80°C for 1 hour and washed 4–5 times until pH = 7) after the catalytic stage before the alkaline treatment.

Bone

Bone sample **K** was washed with distilled water 7 times, dried, and ground on a Freezer/Mill cryogenic homogenizer to obtain 1.538 g of powder. The sample was divided into two parts, with one part (sample **K(2)**) subjected to extraction with dichloromethane at room temperature on an ASETM350 and dried at 70°C and the second part (sample **K(1)**) left without preliminary

purification from insoluble organic components. Next, 1 M HCl was added to the samples and kept at room temperature (pH about 1–1.5) for 2 days. Then the precipitate was separated from the solution by centrifugation and washed with distilled water until pH = 7 was reached. Collagen was purified with a 0.1 M NaOH solution for 20 minutes until a colorless solution was obtained, then the precipitate was washed with distilled water to pH = 7. The precipitate was again immersed in a 1 M HCl solution for 20 minutes and then washed with distilled water to obtain a suspension with pH = 3. The resulting suspensions were thermostated at 70°C for 24 hours, with solutions separated from the precipitates by centrifugation. Collagen solutions were dried in a FreeZone freeze dryer (Labconco) to obtain collagen powder. The samples were then analyzed for $\delta^{13}\text{C}$, $\delta^{15}\text{N}$, and C/N levels. Afterward, the collagen underwent graphitization using AGE-3 and ACS.

Barley Mash

Barley mash samples **A**, **C**, and **F** were subjected to a modified ABA (acid-base-acid) treatment followed by pulp bleaching with sodium chlorite according to the following procedure. The ground samples were repeatedly treated with a solution of 1 M HCl at 80°C for 1 hour for each treatment until a light yellow solution was obtained. The first solution appeared dark brown, but it became brighter with each subsequent treatment. Then the samples were separated from the solution by centrifugation and washed with distilled water until the pH reached 7. Next, the samples were filled with 0.1 M NaOH solution and kept at 80°C for 30 minutes. The solution turned black-brown and was drained. A fresh 0.1 M NaOH solution was added and kept at 80°C for 30 minutes. The procedure was repeated 2 times until a light yellow solution was obtained. Then, the precipitates of all the samples were washed with distilled water, 1 M HCl was added, and the samples were kept at 80°C for 1 hour. After that, the samples were washed with distilled water until the pH was 7. Samples **C** and **F** yielding intensely colored solutions were again treated with alkali. The resulting precipitates were poured with 0.25 M NaOH and kept at 70°C for 15 minutes. This treatment was repeated twice more. Next, 1 M HCl was added at 80°C and kept for 1 hour. The precipitates were washed with distilled water, 60 μl of 10% sodium chlorite solution and 40 μl of 1 M HCl were added to 20 mL of an aqueous suspension, kept at 60°C, and the procedure was repeated several times until a colorless solution and snow-white cellulose were obtained. The cellulose samples obtained from barley samples were washed with distilled water and dried at 70°C.

Humic Acid

Humic acid samples **B**, **D**, and **O** and cellulose sample **M** were not chemically pre-treated before graphitization.

Graphitization

The conversion of the samples to graphite, including combustion, sorption of carbon dioxide on a selective sorbent, desorption, and catalytic reduction of CO_2 with hydrogen (Figure 1) was performed using the ACS procedure (Lysikov et al. 2018). The combustion of a sample (4–10 mg) on the ACS was conducted in the oxygen flow on an aluminum-copper-chrome catalyst at 900°C to support total oxidation. Immediately after the combustion zone, water vapor was frozen out by an ice-salt mixture at -25°C to avoid CO_2 isotope fractionation in the gas flow. Absorption on the selective CO_2 sorbent, CaO, was performed at 550°C, then the line was evacuated, and the sorbent was moved to a hot zone at 920°C for CO_2 desorption. The released CO_2 was frozen with liquid nitrogen in a quartz or Pyrex tube containing 7–8 mg of $\alpha\text{-Fe}$ powder (Aldrich-325 mesh). The gas pressure was measured, a 20% excess relative to

the stoichiometric amount of hydrogen was introduced, and graphitization was performed at 550°C and a total pressure of about 1.2 bar for 5–6 hours. Prior to this procedure, the tube with Fe-catalyst was evacuated, filled with H₂ to 1 bar, and kept at 550°C for 30 minutes. The cold zone (at room temperature) of the tube contained a desiccant, magnesium persulfate, or silica gel impregnated with sulfuric acid, used to remove the resulting water and shift the equilibrium towards the elemental carbon formation. After the process was completed, 2 mg of the powder was obtained, and 1 mg of the powder was pressed into targets and sent for analysis to the MICADAS-28 or BINP AMS.

Another portions of the same samples were graphitized with an AGE-3 (Wacker et al. 2010), followed by powder pressing into targets for MICADAS-28.

Given that we performed this intercomparison for the first time, we prepared two or even more graphites from most samples provided there was enough material to avoid any doubt in the sample quality. Samples **H**, **L**, and **Q** of single rings and a sample of Kauri wood **I** had enough material only for one device. Thus, we could not prepare graphite targets from them by ACS (Table 1).

Measurements

In addition to the data on $\delta^{13}\text{C}$ for graphite samples from MICADAS-28, the measurements of $\delta^{13}\text{C}$ and $\delta^{15}\text{N}$ (the latter only for the bone sample **K**) for non-graphitized samples were also performed on a Delta-V-Advantage mass spectrometer (Thermo Scientific). These measurements were performed in the continuous helium flow mode (high purity grade 6.0) for the samples weighing 0.150–0.250 mg in CO₂ and N₂, obtained by the decomposition of the substance at 1020°C, relative to CO₂ obtained from the ANU sucrose and IVA Urea standards, respectively, under the same conditions. The results were normalized to the VPDB scale. The reproducibility of the values was at the level of $\pm 0.2\%$. C/N was measured by Flash 2000 (Thermo Scientific) in the continuous helium flow mode (purity grade A/B) for collagen samples weighing 1.5–2.5 mg and decomposed at 850°C, with respect to Urea standard.

AMS measurements for all graphite targets followed a routine measurement sequence designed in MICADAS. OX-I (SRM 4990B) was used as a modern standard material, and Polyethylene STD (BN 268530 Thermo Scientific) was used as a background reference material. The MICADAS-28 results were analyzed using the BATS program (Wacker et al. 2010).

RESULTS AND DISCUSSION

To determine the analysis tactics for wood samples containing several annual rings, we studied macroscopic features of the samples **E**, **G**, **N**, and **P** in reflected light on a Stemi 508 with a camera AxioCam HRC (Carl Zeiss) with 2× and 3.2× magnification to determine the number of rings in the sample. The maximum number of rings in the samples did not exceed 40 pieces, and all annual rings in one sample were averaged for each wood sample during the pre-treatment and the subsequent AMS analyses. Samples **E**, **G**, and **P** were represented by the oak, larch, and oak tree species, respectively. Shown in Figure 2 are the photographs of various tree species sections corresponding to samples **E**, **G**, **N**, and **P**.

Table 1 presents the results on GIRI samples, graphitized by AGE-3 and ACS, and then measured on MICADAS-28 together with data on $\delta^{13}\text{C}$, measured by MICADAS-28 for graphite targets, and by Delta-V-Advantage before graphitization. The $\delta^{13}\text{C}$ data obtained on

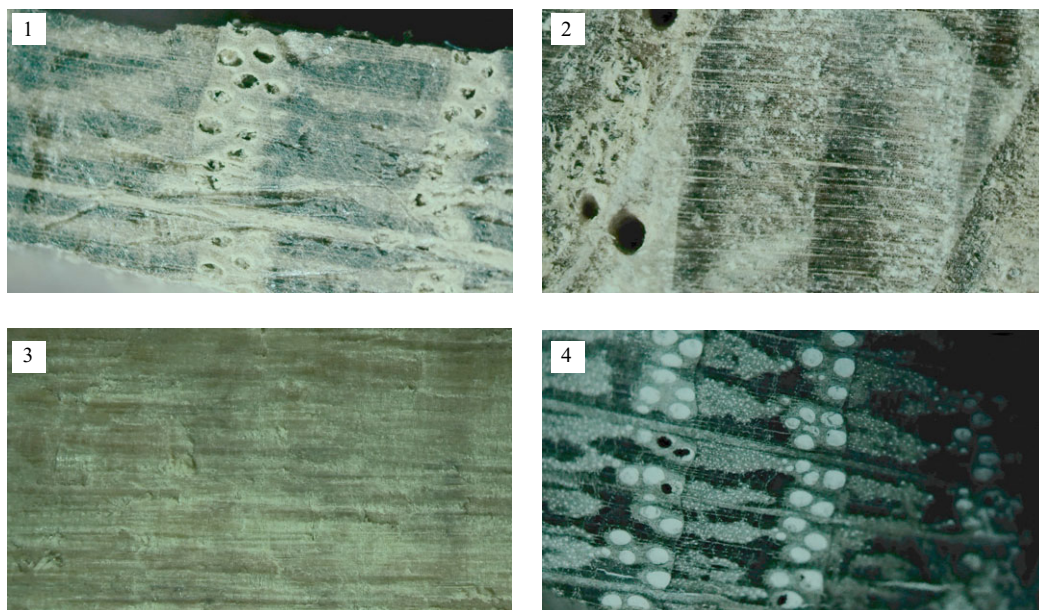


Figure 2 Photograph of sections of GIRI wood samples, taken by the Stemi 508 with a camera AxioCam HRC: 1 – oak (sample E), 2 – larch (sample G), 3 – Kauri wood (sample N), 4 – oak (sample P). Imaging was carried out in reflected light with $2\times$ (1, 4) and $3.2\times$ (2, 3) magnification.

MICADAS-28 for graphites were used for calculating $F^{14}\text{C}$. Since there was no possibility of manual input of fractionation value on MICADAS, no corrections were made for the standard OXI samples. The deviations of $\delta^{13}\text{C}$ measured by MICADAS-28 varied from 0.2 to 3.2 and from 0.2 to 22‰ for graphite targets, made on AGE-3 and ACS, respectively, showing that concentrating CO_2 by equilibrium sorption from the gas flow (on ACS) gives higher isotopic fractionation than that one by chromatographic separation followed by the collection on the zeolite (on AGE-3). The slight variations in $\delta^{13}\text{C}$ measurements between MICADAS-28 and Delta-V-Advantage indicate that isotopic fractionation does not significantly affect the chromatographic concentration of CO_2 followed by graphitization. We noticed that if water was not removed from the gas stream after burning the samples, the isotope fractionation could reach 40% relative to the initial concentration of ^{14}C due to the isotope separation in the gas stream and sorbent capture of only part of the stream: with the head part captured, ^{14}C depletion was observed; with the tail part captured, ^{14}C enrichment was observed. Therefore, for this process to be minimized in the ACS, after combusting the sample, water was frozen out with a salt mixture at approximately -25°C . To account for the significant variations in the isotopic shift in the graphites obtained from ACS, we prepared several samples from one sample at this facility, if possible, to obtain an average of the $F^{14}\text{C}$ values. The issue of “memory” or cross-contamination on the ACS is not as acute as it is on AGE-3 due to two reasons. Firstly, CaO is a material with meso- and macropores ($d > 2 \text{ nm}$), which does not impose diffusion restrictions on CO_2 , unlike zeolite with micropores $< 1 \text{ nm}$. Secondly, CaO can be easily and daily substituted with a fresh portion of the material.

It can be seen from Table 1 that for most GIRI samples, the discrepancy between repeated measurements of graphites after both graphitization methods is less than the 1-sigma uncertainty for a single measurement. The sigma was adjusted according to the deviations in

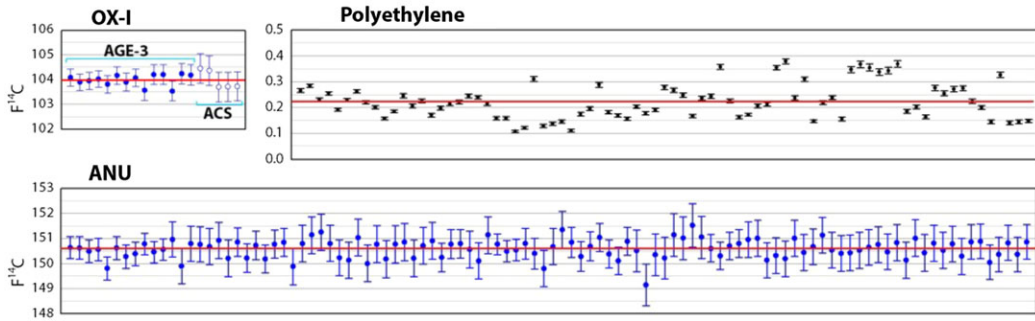


Figure 3 ¹⁴C (×100), measured on MICADAS-28, for the oxalic acid (OX-I) standard, graphitized on AGE-3 and ACS, blank (PE) and sucrose (ANU), graphitized on AGE-3 (red line shows mean values).

repeated measurements of graphites obtained from OXI. Interestingly, the deviation depends to some extent on the type of substance being graphitized. In the course of our work, we came to the conclusion that oxalic acid had the greatest discrepancy while coal and collagen had the lowest. However, the reasons for this issue are still unclear. In this regard, when 2–4 graphites for one sample were obtained, ¹⁴C values were averaged by the following way:

$$\bar{F} = \frac{\sum_{i=1}^N F_i / \sigma_i^2}{\sum_{i=1}^N 1 / \sigma_i^2} \tag{1}$$

$$stdev = \sqrt{\frac{1}{\sum_{i=1}^N 1 / \sigma_i^2}} \tag{2}$$

In those cases when *stdev* was less than a variance (*s*) of mean *F*, the error of *F* was taken equal to the *s*:

$$s = \sqrt{\frac{\sum_{i=1}^N (F_i - \bar{F})^2}{N - 1}}. \tag{3}$$

For example, for graphites of sample **B** produced on AGE-3 *stdev* calculated by (2) is 0.0008, and *s* calculated by (3) is 0.0002, while for graphites produced on ACS *stdev* calculated by (2) is 0.0024, and *s* calculated by (3) is 0.0029 (Table 1S). Formula (2) was used for samples **A, B, D, E, F, H, J, M, Q, O, P**, while formula (3) was used for samples **G, I, K, L** and **N** among the AGE-3 series. Among the ACS series formula (2) was used for samples **D, E, G, K, M, N, O, P**, and formula (3) was used for samples **B** and **C**. Thus, the highest value among the counting, systematic, and experimental deviations was taken as the error of the averaged value of *F*. The initially obtained values of ¹⁴C for individual graphites are presented in Table 1S, and the calculated averaged values of ¹⁴C and radiocarbon ages, produced from these values, – in Table 1.

Given the good convergence of the results obtained for AGE-3 and ACS on GIRI samples (Table 1), as well as the reproducibility of the results for standards (Fig. 3), a simple method of combustion and selective sorption of CO₂ proved to be quite suitable for AMS dating. However, unlike graphites made by AGE-3, the ACS has a limitation in measuring ancient samples: background results of blank samples (polyethylene, PE) were 0.0024 ± 0.0009

(82 measurements) and 0.012 ± 0.003 (5 measurements) for AGE-3 and ACS, respectively. The values of $F^{14}\text{C}$ for PE graphitized by the ACS were 0.0131 ± 0.0002 , 0.0148 ± 0.0002 , 0.0063 ± 0.0001 , 0.0153 ± 0.0002 , and 0.0106 ± 0.0002 . We had only five because we do not usually use the ACS for MICADAS measurements, not including the experiments with GIRI samples. $F^{14}\text{C}$ for ANU standard, graphitized by AGE-3, was 1.5059 ± 0.0037 (104 measurements), which is in perfect agreement with IAEA-C6 value (150.61 pMC).

The most suitable samples for the ACS are biological tissues, sulfurous samples such as oils, bottom sediments, soil samples, ^{14}C labeled substances, and others. The ACS is less affected by impurities, has easily replaceable components, and is easier to maintain. However, due to the relatively high background— $F^{14}\text{C}$ from 0.005 to 0.03 measured by BINP AMS (A.V. Petrozhitskiy et al. 2024), and without special efforts to renew all the components of the ACS and prevent CO_2 excess during its sorption from the flow, the upper limit of the radiocarbon age for routine measurements with ACS does not exceed 35,000 years. For example, the GIRI samples **J** and **M**, prepared by the ACS, were indicated as >35,000 years old. However, the measured fraction modern corrected for background for sample **J** was measured quite adequately (Table 1). The relatively large background fluctuations in the ACS and the need to correct the $F^{14}\text{C}$ for background may lead, in some cases, to a slight sample over aging, such as that observed for sample **K**. Probably the same reason caused some underestimation of the $F^{14}\text{C}$ value in modern samples **A**, **C**, **F**.

CONCLUSIONS

The AMS Golden Valley laboratory has participated in radiocarbon intercomparison for the first time and tested the procedures during the Glasgow International Radiocarbon Intercomparison. Here, we present the results of testing two different graphitization systems with AMS measurement using MICADAS-28. Both systems proved to complement each other perfectly, providing the possibility of measuring ancient and labeled samples, biological tissues, and those contaminated with various impurities, as well as those in various states of aggregation. Based on the simple principles of selective CO_2 sorption, the ACS has been found to be less susceptible to poisoning by sulfur and halogens. However, due to its simple design and inexpensive consumables, this method is most suitable for multiple routine experiments and can be used for the traditional dating of objects no older than 35,000 years. The mean values of the background $F^{14}\text{C}$ were 0.0024 ± 0.0009 and 0.012 ± 0.003 for the AGE-3 and ACS, respectively, both methods giving reproducible results for OXI. The results obtained allow us to recognize the sufficient reproducibility of the results and the remarkable consistency of the experimental determinations.

ACKNOWLEDGMENTS

The work was conducted with the financial support of the Ministry of Science and Higher Education of the Russian Federation: Priority 2030 program, The Russian Academic Excellence Project 5-100, NSU program FSUS-2020-0036, and IAET program FWZG-2022-0007.

The authors are grateful to M.O. Filatova for optical microscopic analyses and to M.A. Kuleshova, O.V. Ershova, U.V. Sryvkina, E.V. Kuznetsova, and K.K. Kuznetsova for their participation in the work. We are especially grateful to Professor Marian Scott for providing the manuscript with preliminary GIRI results and permission to make a comparison.

SUPPLEMENTARY MATERIAL

To view supplementary material for this article, please visit <https://doi.org/10.1017/RDC.2024.46>

REFERENCES

- Arjomand A. 2010. Accelerator mass spectrometry-enabled studies: current status and future prospects. *Bioanalysis* (3):519–541. doi: [10.4155/bio.09.188](https://doi.org/10.4155/bio.09.188)
- Lysikov AI, Kalinkin PN, Sashkina KA, Okunev AG, Parkhomchuk EV, Rastigeev SA, Parkhomchuk VV, Kuleshov DV, Vorobyeva EE, Dralyuk RI. 2018. Novel Simplified Absorption-Catalytic Method of Sample Preparation for AMS analysis designed at the Laboratory of Radiocarbon Methods of Analysis (LRMA) in Novosibirsk Akademgorodok. *International Journal of Mass-spectrometry* 433: 11–18. doi:[10.1016/j.ijms.2018.08.003](https://doi.org/10.1016/j.ijms.2018.08.003)
- Molodin VI, Nenakhov DA, Mylnikova LN, Parkhomchuk EV, Reinhold S, Kalinkin PN, Parkhomchuk VV, Rastigeev SA. 2019. The early neolithic complex on the Tartas-1 site: results of the AMS radiocarbon dating. *Archaeology, Ethnology and Anthropology of Eurasia* 47(1):15–22. doi:[10.17746/1563-0110.2019.47.1.015-022](https://doi.org/10.17746/1563-0110.2019.47.1.015-022)
- Novikov DA, Kopylova YuG, Pyryaev AN, Maksimova AA, Derkachev AS, Sukhorukova AF, Dultsev FF, Chernykh AV, Khvashchevskaya AA, Kalinkin PN, Petrozhitskiy AV. 2023. Radon-rich waters of the Tulinka aquifers, Novosibirsk, Russia. *Groundwater for Sustainable Development* 20:100886. doi:[10.1016/j.gsd.2022.100886](https://doi.org/10.1016/j.gsd.2022.100886)
- Parkhomchuk VV, Rastigeev SA. 2011. Accelerator mass spectrometer of the center for collective use of the Siberian Branch of the Russian Academy of Sciences. *Journal of Surface Investigation* 5(6):1068–1072. doi:[10.1134/S1027451011110140](https://doi.org/10.1134/S1027451011110140)
- Parkhomchuk EV, Gulevich DG, Taratayko AI, Baklanov AM, Selivanova AV, Trubitsyna TA, Voronova IV, Kalinkin PN, Okunev AG, Rastigeev SA, Reznikov VA, Semeykina VS, Sashkina KA, Parkhomchuk VV. 2016. Ultrasensitive Detection of Inhaled Organic Aerosol Particles by Accelerator Mass Spectrometry *Chemosphere* 159:80–88. doi:[10.1016/j.chemosphere.2016.05.078](https://doi.org/10.1016/j.chemosphere.2016.05.078)
- Parkhomchuk EV, Prokopyeva EA, Gulevich DG, Taratayko AI, Baklanov AM, Kalinkin PN, Rastigeev SA, Kuleshov DV, Sashkina KA, Parkhomchuk VV. 2019. Ultrafine organic aerosol particles inhaled by mice at low doses remain in lungs more than half a year. *Journal of Labelled Compounds and Radiopharmaceuticals* 9(62):NS11:785–793. doi:[10.1002/jlcr.3788](https://doi.org/10.1002/jlcr.3788)
- Parkhomchuk EV, Petrozhitskiy AV, Ignatov MM, Kuleshov DV, Kalinkin PN, Prokopyeva EA, Kutnyakova LA, Parkhomchuk VV. 2022. Accelerator mass-spectrometer for biomedical applications (short review), Research trajectory - man, nature, technology, in Russian. 1(6):61–77. doi:[10.56564/27825264_2022_1_61](https://doi.org/10.56564/27825264_2022_1_61)
- Petrozhitskiy AV, Parkhomchuk EV, Ignatov MM, et al. 2024. Comparative features of BINP AMS and MICADAS facilities working at AMS Golden Valley, Russia. *Radiocarbon*. Published online. p. 1–10. doi:[10.1017/RDC.2024.4](https://doi.org/10.1017/RDC.2024.4)
- Rudaya N, Krivonogov S, Slowinski M, Cao X, Zhilich S. 2020. Postglacial history of the Steppe Altai: Climate, fire and plant diversity. *Quaternary Science Reviews* 249:106616. doi:[10.1016/j.quascirev.2020.106616](https://doi.org/10.1016/j.quascirev.2020.106616)
- Sabrekov AF, Terentjeva IE, McDermid GJ, Litt YV, Prokushkin AS, Glagolev MV, Petrozhitskiy AV, Kalinkin PN, Kuleshov DV, Parkhomchuk EV. 2023. Methane in West Siberia terrestrial seeps: origin, transport, and metabolic pathways of production. *Global Change Biology*. Accepted. doi: [10.1111/gcb.16863](https://doi.org/10.1111/gcb.16863)
- Scott EM, Naysmith P, Dunbar E. 2023. Preliminary results from Glasgow International Radiocarbon Intercomparison. *Radiocarbon*. Published online. p. 1–8. doi:[10.1017/RDC.2023.64](https://doi.org/10.1017/RDC.2023.64)
- Synal HA. 2013. Developments in accelerator mass spectrometry. *International Journal of Mass Spectrometry* 349–350:192–202. doi:[10.1016/j.ijms.2013.05.008](https://doi.org/10.1016/j.ijms.2013.05.008)
- Synal HA, Stocker M, Suter M. 2007. MICADAS: A new compact radiocarbon AMS system. *Nuclear Instruments and Methods in Physics Research Section B: Beam Interactions with Materials and Atoms* 259(1):7–13. doi:[10.1016/j.nimb.2007.01.138](https://doi.org/10.1016/j.nimb.2007.01.138)
- Wacker L, Nemeč M, Bourquin J. 2010. A revolutionary graphitisation system: fully automated, compact and simple. *Nuclear Instruments and Methods in Physics Research Section B: Beam Interactions with Materials and Atoms* 268:931–934. doi:[10.1016/j.nimb.2009.10.067](https://doi.org/10.1016/j.nimb.2009.10.067)